Available online at www.sciencedirect.com
SCIENCE DIRECT
Tetrahedron: Asymmetry
Tetrahedron: *Asymmetry* 17 (2006) 1743–1748

Enantiodifferentiation of a silane and the analogous hydrocarbon by the dirhodium method—silane···dirhodium complex interaction

Edison Díaz Gómez,[a] Dieter Albert,[a] Jens Mattiza,[a] Helmut Duddeck,[a,*] Julian Chojnowski[b] and Marek Cypryk[b]

[a]*Institut für Organische Chemie der Universität Hannover, Schneiderberg 1B, D-30167 Hannover, Germany*
[b]*Centre of Molecular and Macromolecular Studies of Polish Academy of Sciences, Department of Heteroorganic Polymers, Sienkiewicza 112, PL-90-363 Łódź, Poland*

Received 18 May 2006; accepted 30 May 2006

Abstract—Chiral silane **1** was enantiodifferentiated by recording NMR spectra in the presence of the chiral dirhodium complex $Rh_2^{(II)}$[(*R*)-(+)-MTPA$_4$] (**Rh***). This is the first report of direct chiral recognition by spectroscopic methods with this class of compounds. A comparison with the carba-analogue **2** shows that **1** is a soft Lewis-base ligand and that the Si–H hydrogen is the binding site, presumably by forming an adduct with a (3c-2e) silicon–hydrogen–rhodium contact (end-on), which exists in equilibrium with the free ligands.

1. Introduction

Chiral silanes play an important role in modern synthetic organic chemistry, for example, in intramolecular Si→C chirality transfer[1] or in catalyzed hydrosilylation reactions.[2] Thus, a easy spectroscopic method for direct observation of a diastereomeric interaction between enantiomeric silane molecules and an enantiopure NMR auxiliary is desirable.

The application of chiral lanthanide shift reagents (CLSR) was introduced several decades ago but this method is restricted to hard Lewis-base ligands, such as carbonyls, amines, alcohols as well as some others.[3] Over the last decade however, we introduced the dirhodium method of chirality recognition in which a chiral enantiopure dirhodium complex $Rh_2^{(II)}$[(*R*)-(+)-MTPA$_4$] (**Rh***: MTPA–H = methoxytrifluoromethylphenylacetic acid ≡ Mosher's acid; see Scheme 1) is added to a $CDCl_3$ solution followed by recording a ^{1}H NMR spectrum.[4] It turned out during the course of this project[5] that soft-base functionalities are particularly suitable for forming relatively stable adducts to **Rh***. As a result, we decided to subject chiral silane **1** (Scheme 1) to the dirhodium experiment in order to determine whether or not this molecule is basic enough to interact with the dirhodium complex. For comparison, we prepared the corresponding carba-analogue **2** (Scheme 1) in order to see how this hydrocarbon behaves under the same NMR experimental conditions.

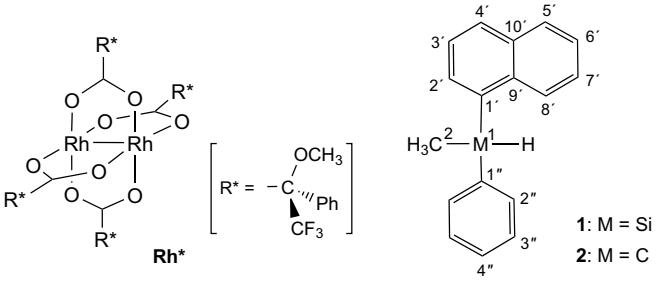

Scheme 1. Structures of the dirhodium complex **Rh***, the chiral silane **1** and its carba-analogue **2**.

2. Results and discussion

2.1. Synthesis, properties and NMR spectroscopy of methyl-1-naphthylphenylsilane 1 and 1-(1-phenylethyl)naphthalene 2

The chiral silane used, (+)-methyl-1-naphthalenylphenylsilane **1**, has been synthesized before; $[\alpha]_D^{20} = +33.4$

* Corresponding author. Tel.: +49 511 762 4615; fax: +49 511 762 4616; e-mail: duddeck@mbox.oci.uni-hannover.de

0957-4166/$ - see front matter © 2006 Elsevier Ltd. All rights reserved.
doi:10.1016/j.tetasy.2006.05.030

corresponding to the (*R*)-configuration at the silicon atom.[6] Alternative pathways to prepare non-racemic **1** have been described,[7] and further studies have confirmed this stereochemical assignment.[8] The sample of **1** used in the dirhodium experiments (see below) had an ee of 22%.

The carba-analogue 1-(1-phenylethyl)naphthalene **2** was prepared by a new route described in the Experimental starting from 1-acetylnaphthalene via α-methyl-α-phenyl-naphthalenemethanol and 1-(1-phenylethenyl)naphthalene. All compounds were identified by IR, NMR and MS and by comparison with reported data.[9,10]

All ^{1}H and ^{13}C NMR signals of **1** and **2** were assigned unequivocally by applying two-dimensional NMR correlation spectroscopy (COSY, HMQC and HMBC).[11] Some severe signal overlap occurred in the presence of **Rh***, particularly for the phenyl signal, so that their exact position could not be identified safely. These nuclei were excluded from the discussion in the following sections.

2.2. Complex formation of 1 and 2 with Rh*

Ligand molecules can form 1:1- and/or 2:1-adducts with the enantiopure dirhodium complex (**Rh***) depending on the relative molar ratio of **L** versus **Rh*** used.[5] All adducts—except those of phosphane ligands (category I)—are kinetically labile so that room-temperature NMR signals are averaged.[5] The equilibria of complex formation are strongly dependent upon the binding energy so that three further categories, II–IV, can be discerned depending on the stabilization of the ligand molecules by adduct formation. In category-II ligands, the binding energy is high, and equilibria are strongly shifted towards the adducts. The equilibria are approximately balanced for category-III-ligands and driven towards free ligands in category-IV-ligands (low or even zero binding energy).[5]

The time-averaged NMR signals of those ligands (categories II–IV)[5] are shifted to some extent when compared to those of the free ligands. In general, such complexation shifts Δδ are small or even negligible. Only if the complexation site is close-by, can noticeable deshielding Δδ-values may be observed because the inductive through-bond effect of the ligand's functional group is enhanced by complexation. Thus, Δδ-values are good indicators for the preferred complexation site. Negative, that is shielding, complexation effects are often observed as well. This can be attributed to through-space anisotropy effects of the various aromatic rings in the adduct.[5]

Complexation shifts obtained for **1** and **2** are presented in Table 2. It was expected that the silane **1** and its carba-analogue **2** are category-IV ligands because they are very weak Lewis bases. Correspondingly, most Δδ-values are small, with only a few nuclei displaying noticeable complexation shifts. Nonetheless, there are some trends, which are visualized in Scheme 2: ^{1}H; dashed circles: $\Delta\delta > 0.1$ ppm, open circles: $\Delta\delta = 0.06$–0.09 ppm; no circles $\Delta\delta \leqslant 0.05$ ppm (insignificant). $^{29}Si/^{13}C$; dashed circles: $\Delta\delta > 0.5$ ppm, open circles: $\Delta\delta = 0.1$–0.5 ppm; no circles $\Delta\delta \leqslant 0.1$ ppm (insignificant).

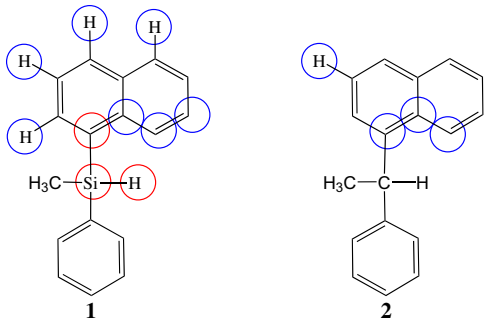

Scheme 2. Strong (red circles) and weak (blue circles) complexation shifts Δδ in **1** and **2**; unmarked atoms show no significant Δδ-values (for details, see text and Table 1).

It is obvious that the two molecules have a completely different binding mode to **Rh***. In **1**, only the silicon nucleus and the hydrogen directly attached (H-1) show strong signal shifts, proving that H-1 is the favourable binding site. All other effects are small, if not even negligible so that a noticeable contribution from the aromatic moieties must be excluded. In contrast, all Δδ-effects are extremely small in the case of the hydrocarbon **2**; only some weak effects can be identified at the naphthalene atoms.

It is interesting to note that the changes in the relevant coupling constants (see captions of Tables 1 and 2) point into the same direction. In the ligated **1**, there is a considerable reduction of the one-bond coupling involving the binding hydrogen H-1 and silicon [$^{1}J(^{29}Si,^{1}H)$] by adduct formation from 194.2 to 184.7/183.5 Hz. A corresponding change of the one-bond $^{13}C,^{1}H$ coupling constant [$^{1}J(^{13}C,^{1}H)$] in **2** does not exist; the values are 126.6 and 126.3 Hz, respectively.

Table 1. ^{1}H, ^{13}C and ^{29}Si chemical shifts (δ, in ppm) of the silane **1** and its carba-analogue **2**, recorded in $CDCl_3$; in ppm relative to internal tetramethylsilane

	1		2	
	δ(^{1}H)	δ(M)[a]	δ(^{1}H)	δ(^{13}C)
1	5.354[b]	−19.8[c]	4.919[d]	40.5
2	0.753	−4.5	1.761	22.5
1′	—	133.3	—	141.5
2′	7.734	135.2	7.425	124.3
3′	7.465	125.2	7.440	125.4
4′	7.898	130.5	7.735	127.0
5′	7.851	128.9	7.834	128.8
6′	7.444	125.6	7.459	125.3
7′	7.417	126.0	7.408	125.8
8′	8.051	128.0	8.032	124.0
9′	—	137.1	—	131.7
10′	—	133.2	—	134.0
1″	—	135.4	—	146.6
2″/6″	7.567	134.9	7.234	127.6
3″/5″	7.337	128.0	7.219	128.4
4″	7.370	129.5	7.148	126.0

[a] M = ^{13}C, except atom 1 (^{29}Si).
[b] $^{1}J(^{29}Si,^{1}H) = 194.2$ Hz; $^{3}J(^{1}H,^{1}H) = 3.9$ Hz.
[c] $^{1}J(^{29}Si,^{13}CH_3) = 53.5$ Hz.
[d] $^{1}J(^{13}C,^{1}H) = 126.6$ Hz; $^{3}J(^{1}H,^{1}H) = 7.1$ Hz.

Table 2. ^{1}H, ^{13}C and ^{29}Si complexation shifts ($\Delta\delta$, in ppm) of the silane **1** and its carba-analogue **2**, recorded in $CDCl_3$[a]

Atom	1		2	
	$\Delta\delta(^{1}H)$	$\Delta\delta(M)$[b]	$\Delta\delta(^{1}H)$	$\Delta\delta(M)$[b]
1	0.31/0.26[c]	1.87/1.70[d]	−0.01/−0.02[e]	−0.01
2	0.04/0.03	0.00	−0.02	−0.03/−0.04
1′	—	0.68	—	0.12/0.10
2′	0.06	ca. −0.1	0.03	0.08/0.07
3′	0.08	ca. −0.1	0.06/0.05	−0.09/−0.11
4′	0.07	−0.04	0.04	−0.10/−0.15
5′	0.09	−0.48/−0.49	0.04	−0.04/−0.09
6′	0.05	ca. −0.5	0.02	−0.11/−0.15
7′	0.02	0.21/0.17	0.02	0.01/0.00
8′	0.05	0.49	0.02	0.11/0.09
9′	—	0.18/0.10	—	0.10/0.08
10′	—	0.07/0.05	—	0.07
1″	—	0.07/0.05	—	0.04/0.03
2″/6″	0.04	0.05	n.d.[f]	0.04
3″/5″	0.00	0.00	0.02	−0.15
4″	0.01	0.05	0.00	−0.03

[a] Two entries if the signal dispersion (Table 3) exceeds 0.01 ppm.
[b] M = ^{13}C, except atom 1 (^{29}Si).
[c] $\Delta^{1}J(^{29}Si,^{1}H) = -9.5/-10.7$ Hz.
[d] $\Delta^{1}J(^{29}Si,^{13}CH_3) = \sim 0$ Hz.
[e] $\Delta^{1}J(^{13}C,^{1}H) = -0.3$ Hz; $\Delta^{3}J(^{1}H,^{1}H) = -0.1$ Hz.
[f] Not detectable.

These divergences in the adduct formation behaviour of **1** and **2** originate from the different electron distribution within the Si–H versus the C–H bond (Scheme 3). In the Si–H bond of **1**, the electrostatic (Mulliken) charges, as calculated by density-functional methods, are +0.386 (Si) and −0.101 (H) whereas the corresponding values for the C–H bond of **2** are +0.054 (C) and +0.091 (H). Moreover, the dipole moment of **1** (0.78 D) is nearly parallel to the Si–H bond whereas that of **2** (0.16 D) is much lower and, furthermore, points into the cavity opened by the two aromatic ring systems, thereby, having a strong component antiparallel to the C–H bond (Scheme 3).

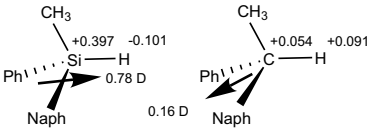

Scheme 3. Electrostatic (Mulliken) charges of the atoms in the Si–H bond of **1** (left) and the respective C–H bond of **2** (right) as well as dipole moments (in Debye), as calculated by density-functional calculations (B3LYP, 6-31G*).

It has been shown in a theoretical study[12] that the binding between a dirhodium tetracarboxylate complex and a ligand is accomplished primarily by two interactions: (a) electrostatic attraction and (b) HOMO–LUMO interaction; the electrostatic attraction prevails. In essence, this factorization of interaction contributions has been qualitatively confirmed by our earlier dirhodium experiments although we found that there is, in addition, a steric repulsion from the Mosher acid residues if the binding site in the ligand molecule is sterically congested.[5]

Interactions between metal atoms and Si–H bonds have been investigated intensively and were reviewed recently.[13] It has been shown that the $^{1}J(^{29}Si,^{1}H)$ coupling constant in particular is a very sensitive probe for this interaction because it is reduced enormously from more than 190 Hz in the free silane to 30–70 Hz in a kinetically stable silane σ-complex. Based on those findings,[13] two different kinds of Si–H–Rh contacts are conceivable for the present case:

(a) The two adduct components **Rh*** and **1** exist in a fast-exchange equilibrium with species **A** (side-on; Scheme 4) while the observed reduction of the $^{1}J(^{29}Si,^{1}H)$ coupling constant of ca. 10 Hz indicates a predominance of the free components (6–10% for the σ-complex), a behaviour typical of category-IV ligands (as stated above).
(b) The interaction is essentially a three-centre-two-electron binding (3c-2e) as represented by species **B** (end-on; Scheme 4). Thus, the Si–H bond order is somewhat reduced, again time averaged, leading to a decrease of the $^{1}J(^{29}Si,^{1}H)$-value.

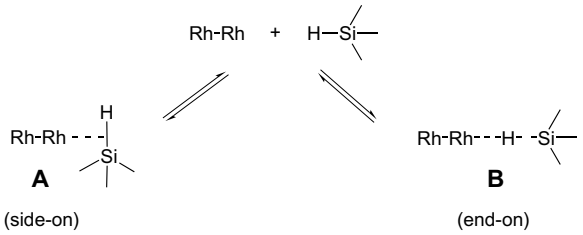

Scheme 4. Conceivable interaction mechanisms between the rhodium atoms in **Rh*** and the silicon–hydrogen bond; **Rh*** is represented by 'Rh–Rh'.

An evaluation of all the arguments and an inspection of all the other data in Table 2 led to the following interpretation: the hydridic nature of H-1 in the silane **1** makes this atom a soft Lewis base and enables it to act as a weak, but significant, binding site (category-III or -IV ligand). The ligand approach to **Rh*** is supported by the electrostatic properties of the Si–H bond and the favourable orientation of the dipole moment. The change in the $^{1}J(^{29}Si,^{1}H)$-value suggests that, at least to some extent, an additional orbital interaction exists. Species **B** is more reasonable than species **A**. The silane σ-complex **A** involves a much closer contact between the aromatic residues of both components, **1** and **Rh***, than species **B** and this should result in significant ^{1}H and ^{13}C shieldings due to mutual anisotropic effects. However, none such effects are visible in the data body of Table 2.

Apparently, the C–H bond of the hydrocarbon **2**, which corresponds to the Si–H bond of **1**, does not contribute at all to any binding. This is not surprising because interaction models as outlined in Scheme 4 are not valid here.[13] The C–H bond in **2** shows no Lewis basicity and its electrostatic properties favour an approach of the naphthalene π-electron system, which, according to a density-functional calculation, bears the largest electron density. Altogether, **2** is an extremely weak ligand (category IV); however, as

will be shown in the next section it is still strong enough to profit from diastereomeric interactions with **Rh*** enabling chiral recognition.

2.3. Diastereomeric dispersions and chiral recognition

Beside the complexation shift $\Delta\delta$, the second parameter extractable from the dirhodium experiments is the diastereomeric dispersion effect Δv, which provides chiral recognition; in principle, all nuclei in the free chiral ligand molecules become diastereotopic in the adducts. Hence, the signal of a given ligand nucleus is split into two anisochronous signals, while the chemical shift difference is the dispersion Δv. The relative signal areas (integrals) represent the ratio of the enantiomers. Since such values are mostly in the range of 1–100 Hz, we prefer to calibrate them in Hertz. The reader should be aware, however, that the magnitudes of these values depend linearly on the external field B_0, here 9.4 T (Table 2).

Whereas the sample of **2** was racemic, that of **1** used in the dirhodium experiments had an $[\alpha]_D^{20} = +13.1$ corresponding to an ee of 22% [(+)-R_{Si}:(−)-S_{Si} = 61:39].[6–8] This is well reflected by the relative intensities in the ^{1}H and ^{29}Si NMR signal sets (see Fig. 1).

All diastereomeric dispersion effects (Δv) on the NMR signals of **1** and **2** are compiled in Table 3. For some signals, Δv-values could not be identified safely due to signal overlap, and the corresponding entry in Table 3 was marked by 'n.d.' (not detectable). On the other hand, a number of signals were not split; their dispersion is too low to be resolved. As a result, their Δv-values were notified by '0'. For those signals of **1**, however, where both signals and their differential intensities could be identified, the signs of the Δv-values were determined according to the following definition: $\Delta v = \Delta v[(+)\text{-}R_{Si}] - \Delta v[(-)\text{-}S_{Si}]$.

It can be seen, from both Figure 1 and Table 3, that an enantiodifferentiation of both ligands **1** and **2** is easily possible by the direct measurement of their NMR signals and by their integration. Enough nuclei are available in both cases. To the best of our knowledge, this is the first report of direct spectroscopic enantiodifferentiation of silanes. However, it should be noted that, recently, Oestreich et al. described the use of HPLC with chiral stationary phases for this purpose.[14]

Table 3. ^{1}H, ^{13}C and ^{29}Si dispersion effects (Δv, in Hz) of the silane **1** and its carba-analogue **2** at 9.4 T (400.1 MHz ^{1}H, 100.6 MHz ^{13}C, and 79.5 MHz ^{29}Si), recorded in $CDCl_3$. Signs of Δv-values (for **1** only) are defined according to the equation: $\Delta v = \Delta v[(+)\text{-}R_{Si}] - \Delta v[(-)\text{-}S_{Si}]$

Atom	1		2	
	$\Delta v(^1H)$	$\Delta v(M)$[a]	$\Delta v(^1H)$	$\Delta v(M)$[a]
1	−17	−14	3	0
2	−4	0	0	1
1′	—	0	—	2
2′	0	n.d.[b]	n.d.	1
3′	n.d.	n.d.	3	2
4′	0	0	0	5
5′	0	+1	0	5
6′	n.d.	n.d.	n.d.	4
7′	n.d.	−4	n.d.	1
8′	0	n.d.	0	1
9′	—	−3	–	1
10′	—	+3	—	0
1″	—	−2	—	1
2″/6″	0	0	n.d.	0
3″/5″	n.d.	0	n.d.	0
4″	n.d.	−1	n.d.	0

[a] M = ^{13}C, except atom 1 in **1** (^{29}Si).
[b] n.d.: not detectable.

It is worth mentioning that another method of chiral recognition has been reported for aromatic hydrocarbons involving mononuclear rhodium complexes.[15] In addition, the use of a CLSR-related method for differentiating aromatic hydrocarbon enantiomers has been reported more than 20 years ago (addition of Ag^+ salts).[16] However, it should be kept in mind that the latter are three-component-experiments and it is not easy to find a proper experimental set-up.

At this stage, it is not yet clear whether a correlation rule for the determination of the absolute configuration may emerge, a rule analogous to those described by us previously for some spirochalcogenuranes[17] and phospholene chalcogenides.[18] More chiral silane compounds are required to answer this question.

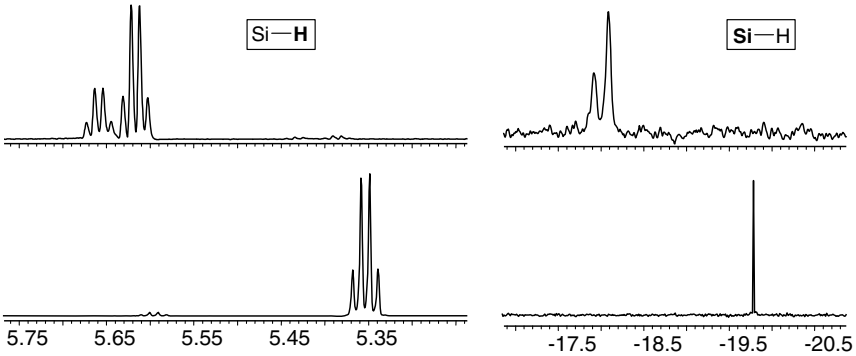

Figure 1. ^{1}H (left) and ^{29}Si NMR spectral sections (right) of the silane **1**; bottom: normal spectra of the free silane, top: spectra in the presence of an equimolar amount of **Rh***.

3. Conclusion

It has been shown that chiral silane **1** can be enantiodifferentiated easily by recording the NMR spectra in the presence of an equimolar amount of the chiral dirhodium complex **Rh*** observing changes in the chemical shifts (complexation shifts, $\Delta\delta$) and coupling constants, as well as signal splittings (diastereomeric dispersions, $\Delta\nu$). Due to its hydridic nature, the hydrogen atom attached to the silicon atom acts as a weak Lewis base, presumably, by interacting in a three-centre-two-electron (3c-2e) binding to one rhodium atom of **Rh*** in the axial position. This interpretation is supported by the completely different behaviour of the carba-analogue **2** in an analogous dirhodium experiment.

This is the first report of direct spectroscopic chiral recognition of silanes lacking any further Lewis-basic heteroatom functionality.

4. Experimental

4.1. Substances

The syntheses of **Rh***[4] and **1**[6] [ee = 22%; (+)-R_{Si}:(−)-S_{Si} = 61:39] have been described before.

4.1.1. 1-(1-Phenylethenyl)naphthalene. 1-Acetylnaphthalene (1 g, 5.9 mmol) was dissolved in 25 ml dried THF and cooled to −78 °C. Phenyllitihium (3 ml) was added dropwise with stirring in an inert gas atmosphere. The solution was further stirred at −78 °C for 30 min and then warmed to room temperature. Ice-water was added, the organic phase separated, dried over Na_2SO_4, filtered and the solvent evaporated in vacuo. The resulting α-methyl-α-phenyl-naphthalenemethanol, a yellowish oil, contained a small amount of the starting material (1-acetylnaphthalene), as proven by the carbonyl band ($\tilde{\nu}$ = 1681 cm^{-1}) in the IR spectrum of the crude product. Nevertheless, the crude α-methyl-α-phenyl-naphthalenemethanol was subjected to water elimination without further purification by dissolving it in 25 ml of methanol with a catalytic amount of *p*-toluenesulfonic acid and refluxing for two hours. After evaporation of the solvent, a yellow viscous liquid was obtained, which was chromatographed on silica gel with *n*-hexane and ethylacetate (16:1). After drying, 1-(1-phenylethenyl)naphthalene (195 mg, 0.9 mmol, 15% yield relative to 1-acetylnaphthalene) was isolated and identified by comparison of its spectral properties with literature data.[9] This reaction sequence was not optimized for yield.

4.1.2. 1-(1-Phenylethyl)naphthalene 2. 1-(1-Phenylethenyl)-naphthalene (195 mg; 0,9 mmol) was dissolved in 25 ml of tetrahydrofurane with a catalytic amount of palladium/charcoal under a nitrogen atmosphere. Hydrogen was added under stirring for 24 h. Then, the mixture was filtered off, evaporated and chromatographed on silica gel with *n*-hexane and ethyl acetate (8:1). After evaporation of the eluant and drying in vacuo for 48 h, 1-(1-phenylethyl)naphthalene **2** (175 mg, 0.76 mmol, 84% yield) was obtained as a crystalline solid.[10] IR (solid state) ($\tilde{\nu}$, cm^{-1}) 3054, 1660, 1592, 1491, 1252, 1024, 907, 774, 694. EI-MS *m*/*z* (rel. int.) 232 (M^+, 85), 217 (100), 215 (69), 202 (62), 189 (11), 155 (20), 143 (15), 128 (16), 115 (19), 108 (39), 91 (24), 77 (17), 51 (9). HRMS 232.1252; calcd for $C_{18}H_{16}$ 232.1252. For the NMR spectra (see Table 1).

4.2. NMR spectroscopy

^{1}H (400.1 MHz) and ^{13}C NMR spectra (100.6 MHz) were performed on a Bruker Avance DPX-400 spectrometer, the ^{29}Si NMR spectra were recorded at 79.5 MHz in the direct mode on the same instrument. Chemical shift standards were internal tetramethylsilane (δ = 0 ppm) for ^{1}H, ^{13}C and ^{29}Si. ^{1}H and ^{13}C signal assignments are based on DEPT and two-dimensional COSY, HMQC and HMBC spectra (standard Bruker software). Digital resolutions were 0.14 Hz/point in the ^{1}H, 0.24 Hz/point in the ^{13}C and 0.49 Hz/point in the ^{29}Si NMR spectra.

In the standard dirhodium experiment, **Rh*** and an equimolar amount of the ligands **1** or **2**, respectively, were dissolved in 0.7 ml $CDCl_3$. Typically, 48.6 mg of **Rh*** (0.043 mM concentration) were employed. No acetone–d_6 was added for assisting **Rh*** solubility[19] in order to avoid competition of the acetone molecules with ligands **1** and **2** in the adduct formation.[5] Instead, the dissolution process was accelerated by exposing the NMR sample tubes to an ultrasonic bath.

4.3. Calculations

Density-functional calculations (B3LYP, 6-31G*) of the free ligands were performed using Spartan '04 (Wavefunction® software package).

Acknowledgements

This work has been performed within the project 'Biologically Active Natural Products: Synthetic Diversity' (Department of Chemistry, Hannover University) and was supported by the Deutsche Forschungsgemeinschaft.

References

1. Oestreich, M. *Chem. Eur. J.* **2006**, *12*, 30–37.
2. See for example: (a) Brunner, H. *Angew. Chem., Int. Ed.* **2004**, *43*, 2749–2750; (b) Yamamoto, K.; Hayashi, T. Hydrosilylations: Hydrosilylation of Olefins. In *Transition Metals for Organic Synthesis*, 2nd ed.; Beller, M., Bolm, C., Eds.; Wiley-VCH Verlag: New York, 2004; Vol. 2, pp 167–181.
3. (a) Sullivan, G. R. *Top. Stereochem.* **1978**, *10*, 287–329; (b) Rinaldi, P. L. *Progr. NMR Spectrosc.* **1983**, *15*, 291–352; (c) Parker, D. *Chem. Rev.* **1991**, *91*, 1441–1457; (d) Rothchild, R. *Enantiomer* **2000**, *5*, 457–471.
4. Wypchlo, K.; Duddeck, H. *Tetrahedron: Asymmetry* **1994**, *5*, 27–30.
5. Duddeck, H. *Chem. Rec.* **2005**, *5*, 396–409.
6. (a) Sommer, L. H. *Stereochemistry, Mechanism and Silicon*; McGraw-Hill: New York, 1965; Chapter 2, pp 40–45; (b) Sommer, L. H.; Frye, L.; Parker, A.; Michael, K. W. *J. Am. Chem. Soc.* **1964**, *86*, 3271–3276.

7. (a) Corriu, R. J. P.; Moreau, J. J. E. *Bull. Soc. Chim. Fr.* **1975**, 901–902; (b) Kobayashi, K.; Kato, T.; Masuda, S. *Chem. Lett.* **1987**, 101–104.
8. (a) Cerveau, G.; Colomer, E.; Corriu, R. J. P. *Organometallics* **1982**, *1*, 867–869; (b) Chojnowski, J.; Cypryk, M.; Michalski, J.; Wozniak, L.; Corriu, R.; Lanneau, G. *Tetrahedron* **1986**, *42*, 385–397; (c) Stang, P. J.; Learned, A. E. *J. Am. Chem. Soc.* **1987**, *109*, 5019–5020; (d) Colomer, E.; Corriu, R. J. P.; Marzin, C.; Vioux, A. *Inorg. Chem.* **1982**, *21*, 368–373.
9. (a) Berthiol, F.; Doucet, H.; Santelli, M. *Eur. J. Org. Chem.* **2003**, 1091–1096; (b) Bajracharya, G. B.; Nakamura, I.; Yamamoto, Y. *J. Org. Chem.* **2005**, *70*, 892–897; (c) Xing, D.; Guan, B.; Cai, G.; Fang, Z.; Yang, L.; Shi, Z. *Org. Lett.* **2006**, *8*, 693–696.
10. Gu, W.; Weiss, R. G. *Tetrahedron* **2000**, *56*, 6913–6925.
11. For example: (a) *Two-Dimensional NMR Spectroscopy, Applications for Chemists and Biochemists*; 2nd ed., Croasmun, W. R., Carlson, R. M. K., Eds., VCH: New York, 1994; (b) Nelson, J. H. *Nuclear Magnetic Resonance Spectroscopy*; Prentice-Hall, Pearson Ed.: Upper Saddle River, NJ, 2003.
12. Deubel, D. V. *Organometallics* **2002**, *21*, 4303–4305.
13. Nikonov, G. I. *Adv. Organomet. Chem.* **2005**, *53*, 217–309, and references cited therein.
14. (a) Oestreich, M.; Schmid, U. K.; Auer, G.; Keller, M. *Synthesis* **2003**, 2725–2739; (b) Oestreich, M.; Auer, G.; Keller, M. *Eur. J. Org. Chem.* **2005**, 184–195.
15. Buriak, J. M.; Osborne, J. A. *J. Chem. Soc., Chem. Commun.* **1995**, 689–690.
16. (a) Dambska, A.; Janowski, A. *Org. Magn. Reson.* **1980**, *13*, 122–125; (b) Offermann, W.; Mannschreck, A. *Org. Magn. Reson.* **1984**, *22*, 355–363, and references cited therein.
17. Gáti, T.; Tóth, G.; Drabowicz, J.; Moeller, S.; Hofer, E.; Polavarapu, P. L.; Duddeck, H. *Chirality* **2005**, *17*, S40–S47.
18. Moeller, S.; Drzazga, Z.; Pakulski, Z.; Pietrusiewicz, K. M.; Duddeck, H. *Chirality* **2006**, *17*, 395–397.
19. Meyer, C.; Duddeck, H. *Magn. Reson. Chem.* **2000**, *38*, 29–32.